Steady-state optical modulation spectroscopy of *p*-type *a*-Si:H

H. Herremans and W. Grevendonk
Katholieke Universiteit Leuven, Departement Natuurkunde, Laboratorium voor Halfgeleiderfysica, Celestijnenlaan 200D, B-3001 Heverlee, Belgium
(Received 25 March 1994)

Steady-state optical modulation spectroscopy (OMS) was carried out to obtain information on the gap states of *p*-type hydrogenated amorphous silicon (*a*-Si:H). Doping was achieved by adding diborane (B_2H_6) to the silane (SiH_4) gas in a conventional rf glow-discharge deposition. Measurements were performed at room temperature and at $T \simeq 20$ K. The OMS spectra show clear differences with the spectra of undoped *a*-Si:H. These differences can be associated with the dopant states, lying in the valence-band tail, created by the boron doping. The numerical calculations, based on a model for the density-of-states distribution, take into account several possible optical transitions. The energy positions of the dopant states, B_4^- and B_4^0, and the doping-induced dangling-bond defects, D_B^+ and D_B^0, are determined. The dangling-bond states tend to shift further away from the valence-band edge with increasing doping concentration while the dopant states stay at the same energy position.

I. INTRODUCTION

In 1975, Spear and LeComber demonstrated the possibility of doping *a*-Si:H.[1] Since then, many studies have been undertaken in order to unravel the doping mechanism and the electronic structure of doped *a*-Si:H using several experimental techniques. Also optical modulation spectroscopy (OMS) has contributed to reveal information about this problem.[2–4] Recently, Kočka *et al.*[4] have published a study of the states introduced in *a*-Si:H by phosphorus doping. Boron-doped material received less attention; however, it is known that the optical gap decreases with increasing boron concentration when using B_2H_6 as a dopant gas[5] and that, depending on doping concentration, the D_B^+ dangling bond has an energy position between 1.1 and 1.4 eV with respect to the valence band (VB); these values were obtained using the constant photocurrent method[6,7] and photothermal deflection spectroscopy.[8] Also OMS data are available: Vardeny *et al.*[2] positioned D_B^+ at 0.95 eV while, in a later work, Chen *et al.*[3] obtained an energy position of 1.28 eV above the VB. The aim of this work is to describe OMS spectra of a series of B_2H_6-doped *a*-Si:H samples at room temperature and at low temperature (20 K) and to derive the energy positions of dangling-bond and dopant states. The contributions of the possible optical transitions to the OMS spectrum will be evaluated step by step.

First, in Sec. II, the experimental details of the technique used and the samples are described. In Sec. III the OMS spectra are presented and discussed. A detailed description of our model to determine the energy positions of the gap states is given in Sec. IV. The results of the calculations using this model are presented and discussed in Sec. V. Finally, in Sec. VI, conclusions are summarized.

II. EXPERIMENTAL DETAILS

Steady-state optical modulation spectroscopy contains information on all the gap states, based on the transitions of carriers between these gap states and the band states. By irradiating the sample with laser light of an energy resulting in band-to-band excitation of carriers (pump beam), modulation of the transmission of a probe beam is caused. As a pump beam we use an argon-ion laser with an intensity of 30 $mW\,cm^{-2}$; an incandescent light source functions as the probe beam. The laser beam is chopped with a modulation frequency of 74 Hz. The generated excess carriers, created by the laser illumination, are trapped into the gap states changing their occupancy and resulting in an enhancement (photoinduced absorption) or a reduction (photoinduced bleaching) of the optical transitions. This change in the optical transitions affects the absorption, and thus the transmission, of the probe beam. Therefore, OMS measures the change in absorption coefficient $\Delta\alpha$ due to laser irradiation, which is proportional to minus the relative change in transmission $-\Delta T/T$ (Ref. 9) if the laser intensity is low enough[10] as is the case in our experimental circumstances. More details about this optical technique may be found elsewhere.[2,9,11–14]

The *p*-type *a*-Si:H samples were deposited at the University of Utrecht with the conventional rf glow-discharge method in an ultrahigh vacuum plasma deposition system. The rf power (13.56 MHz) is capacitively coupled to the parallel-plate electrodes in the deposition reactors. The power density equals 113 $mW\,cm^{-2}$. Other deposition parameters are a substrate temperature of 170 °C, a gas pressure of 0.13 mbar, and a total gas flow of 54 SCCM (SCCM denotes cubic centimeter per minute at STP). As gases, pure SiH_4, and 0.1% B_2H_6 diluted in H_2 are used. We investigated three samples with differ-

ent (SiH_4:B_2H_6+H_2) ratios. The films are deposited on Corning 7059 glass substrates.

III. OMS SPECTRA

In Fig. 1, the OMS spectra obtained at room temperature (a) and at $T \simeq 20$ K (b) of the three investigated samples are shown. The inset of Fig. 1(a) represents an example of a spectrum of undoped a-Si:H measured at room temperature. All curves are averages of the interference pattern due to the thin films.

The spectra consist of photoinduced absorption (PA) with an onset at the lower photon energies and photoinduced bleaching (PB), which sets in roughly at the maximum of the spectra, at about 1 eV. At the highest photon energies the curve increases sharply indicating an increased absorption, due to the thermal shift of the absorption edge. Therefore, this part of the spectrum allows us to make a rude estimation of the optical gap parameter E_g. As can be noticed in Fig. 1, the influence of the thermal effect sets in at lower photon energies for samples deposited with higher doping concentration in the gas phase, indicating that the optical gap indeed decreases with increasing doping.

At both temperatures, a decrease in the magnitude of the spectra with increasing doping concentration is observed. A similar effect has been reported for P-doped samples.[3] Because one expects an increase of the defect density,[8,15–21] a decrease of the recombination time with increasing doping must be assumed.

Compared to the spectrum of undoped a-Si:H [inset of Fig. 1(a)], all spectra show a different shape. In undoped a-Si:H, the spectra are composed of one PA and one PB contribution. The PA contribution is ascribed to optical transitions between charged D^- defects, created by laser illumination, and the conduction band (CB), while the PB is associated with optical transitions between neutral D^0 states, emptied by laser illumination, and the CB.[14] In the spectra of p-type a-Si:H more contributions can be distinguished, indicating that other important states besides silicon dangling bonds are involved. Indeed, in boron-doped a-Si:H two kinds of defects are present: the shallow dopant states B_4^- and the deep DB states D_B^+. Therefore, the PA contribution, which is situated at the low photon energies, can be ascribed to a superposition of optical transitions between the VB and B_4^0 states and between D_B^0 states and the CB. The B_4^0 states, as we suppose, are created during laser illumination by trapping excess holes on B_4^- states, while the D_B^0 states are formed by trapping excess electrons on D_B^+ states. Concerning the PB contributions, a first one sets in at about 1 eV associated with optical transitions between the VB and D_B^+ states, and a second one is noticed at about 1.6 eV attributed to optical transitions between B_4^- states and the CB.

Figure 2 shows a comparison between a room-temperature spectrum and data obtained at $T \simeq 20$ K. The room-temperature data are scaled by a factor with respect to the low-temperature data. The main difference is noticed in the range between 1 and 1.6 eV ascribed to optical transitions between the VB and D_B^+ states. No considerable changes are observed in the contributions involving B_4^0 or B_4^- states, which may indicate that the quasi-Fermi level for trapped holes is pinned in p-type a-Si:H.

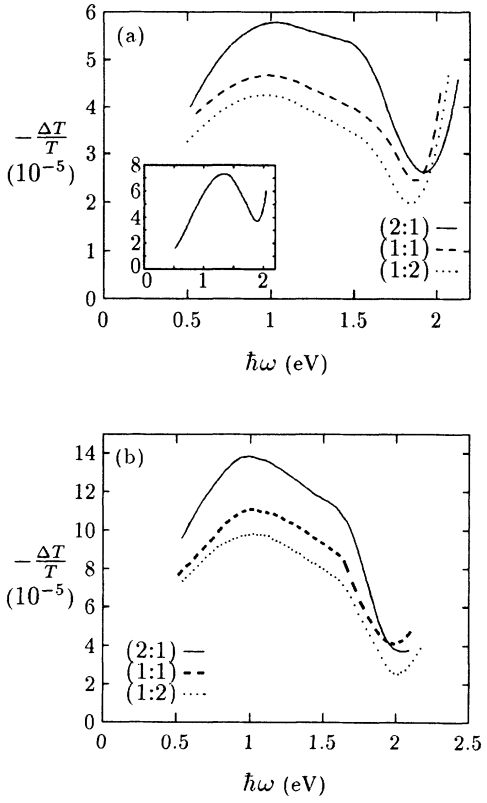

FIG. 1. OMS spectra of the three B-doped a-Si:H samples measured (a) at room temperature and (b) at $T \simeq 20$ K. The values in parentheses represent the (SiH_4:B_2H_6+H_2) ratios. In the inset of (a), an OMS spectrum of undoped a-Si:H is shown.

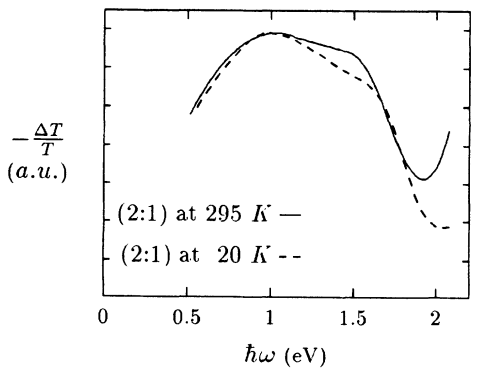

FIG. 2. Room-temperature and low-temperature data of the p-type a-Si:H sample with a (SiH_4:B_2H_6+H_2) ratio of (2:1). The room-temperature values are scaled by a factor of 2.4 with respect to the low-temperature values.

IV. MODELING

To obtain more information on the gap state distributions, in particular the energy positions of the gap states, a model was developed and fitted to our OMS data. This model is based on the possible optical transitions between localized gap states and extended band states.

The absorption of light needed to perform optical transitions from initial states with energy E to final states with energy $E+\hbar\omega$ may be described by the equation

$$\alpha(\hbar\omega) = \frac{C}{\hbar\omega}\int_{-\infty}^{+\infty} |M|^2 g_i(E) g_f(E+\hbar\omega) f(E) \times[1-f(E+\hbar\omega)]dE, \quad (1)$$

where C is a constant, M stands for the momentum matrix element of the optical transitions, and $g(E)$ and $f(E)$ are the density-of-states (DOS) function and the occupancy function, respectively. The integral is taken over all initial states.

Assuming an energy-independent matrix element M and an occupancy function that is changed by laser irradiation $[f(E) \rightarrow f^*(E)]$, the photoinduced change in absorption coefficient may be written as[22]

$$\Delta\alpha(\hbar\omega) = \frac{C|M|^2}{\hbar\omega}\int_{-\infty}^{+\infty} g_i(E) g_f(E+\hbar\omega) \times[\Delta f(E) - \Delta f(E+\hbar\omega)]dE, \quad (2)$$

where $\Delta f(E) = f^*(E) - f(E)$. The occupancy function in the dark $f(E)$ is given by the Fermi-Dirac distribution at equilibrium

$$f(E) = \{1+\exp[(E-E_F)/kT]\}^{-1}, \quad (3)$$

where E_F represents the Fermi energy, k is the Boltzmann constant, and T is the absolute temperature. Under laser illumination the occupancy function becomes

$$f^*(E) = \frac{1-l}{1+\exp[(E-E_{Fp})/kT]} + \frac{l}{1+\exp[(E-E_{Fn})/kT]}, \quad (4)$$

where E_{Fp} and E_{Fn} are the quasi-Fermi levels for trapped holes and electrons, respectively, and l is the constant occupancy between the two quasi-Fermi levels.

In a first step, we have taken into account the possible optical transitions between localized dopant or DB states and extended VB or CB states. The photoinduced absorption $\Delta\alpha$ is then considered to be a sum of four components, two terms include optical transitions involving the VB, the other terms represent optical transitions to the CB

$$\Delta\alpha(\hbar\omega) = C_1\Delta\alpha_{\mathrm{VB}\rightarrow B_4^0}(\hbar\omega) + C_2\Delta\alpha_{D_B^0\rightarrow\mathrm{CB}}(\hbar\omega) + C_3\Delta\alpha_{\mathrm{VB}\rightarrow D_B^+}(\hbar\omega) + C_4\Delta\alpha_{B_4^-\rightarrow\mathrm{CB}}(\hbar\omega). \quad (5)$$

The C_i ($i = 1$ to 4) represent relative proportionality constants. The photoinduced absorption of each contribution $\Delta\alpha_{i\rightarrow f}$ may be expressed as given in Eq. (2), where C is replaced by the above-introduced C_i. The integral is taken between the limits $E_v - \hbar\omega$ and E_c. To be able to make the calculations we still have to define the density-of-states distribution functions. For the VB and CB DOS a parabolic distribution was taken,

$$g_{\mathrm{VB}} = N_v(E_v - E)^{1/2}, \quad (6)$$

$$g_{\mathrm{CB}} = N_c(E - E_c)^{1/2}, \quad (7)$$

where E_v and E_c are the mobility edges and N_v and N_c are constants. A Gaussian distribution is assumed for the dangling-bond and the dopant states

$$g_i = N_i\frac{1}{\sigma_i\sqrt{2\pi}}\exp\left[-\frac{1}{2}\left(\frac{E-\mu_i}{\sigma_i}\right)^2\right]. \quad (8)$$

The Gaussian peaks at μ_i and has a width given by the standard deviation σ_i. The index i stands for DB, respectively, B states. All N_i are given the same value as was suggested by others.[18–20]

In a next step, also optical transitions between the VB tail (VBT) states and the extended band states, either the VB or the CB, are included. An exponential distribution was assumed for the tail states

$$g_{\mathrm{VBT}} = N_{\mathrm{VBT}}\exp(-E/E_0), \quad (9)$$

where E_0 is the exponential band-tail parameter, which represents the width of the tail. Two extra terms are then added to Eq. (5), namely:

$$C_5\Delta\alpha_{\mathrm{VBT}\rightarrow\mathrm{CB}}(\hbar\omega) + C_6\Delta\alpha_{\mathrm{VB}\rightarrow\mathrm{VBT}}(\hbar\omega). \quad (10)$$

The coefficients C_i may be different for each kind of optical transition because optical matrix elements and absolute values of the densities may be different. These coefficients are determined by a least-squares fit to the experimental data. Therefore, we can only determine the relative strengths of the several contributions to the OMS spectrum.

In the numerical calculations, the parameters E_F, E_{Fp}, E_{Fn}, and the energy positions of the Gaussian distributions were taken with respect to the VB (E_v=0 eV). Therefore, $E_c = E_g$. For the gap energy E_g, we had to introduce a value slightly higher than the Tauc gap (see Sec. V).

V. ANALYSIS AND DISCUSSION

Figure 3 shows the results of numerical calculations taking into account some of the optical transitions mentioned above for the sample with the lowest doping concentration and measured at $T \simeq 20$ K. The curves are scaled so that the highest values coincide. When only transitions involving the B_4^- and B_4^0 states are considered, the calculations result in curves like the dashed one of Fig. 3(a). It is clear that besides B_4^- and B_4^0 other states must contribute. At the lower photon energies an extra contribution from $D_B^0 \rightarrow$ CB transitions can be added (PA), while at higher photon en-

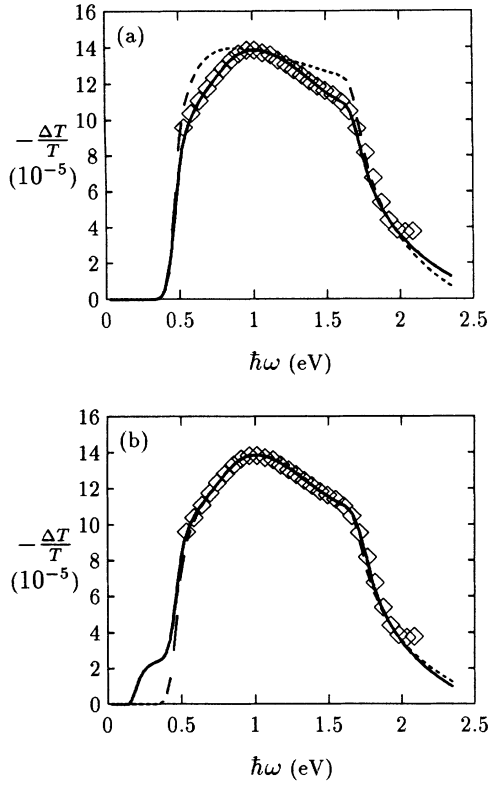

FIG. 3. Experimental ($\diamond$) and calculated $-\Delta T/T$ spectra of the p-type a-Si:H sample with a (SiH_4:B_2H_6+H_2) ratio of (2:1) measured at $T \simeq 20$ K. The curves are scaled so that the highest values coincide. In (a), calculated spectra involving only dopant states (dashed line) and DB's and dopant states (full line) are shown. In (b), calculated spectra involving DB's and dopant states (dashed line) as well as the effect of the extra contribution of VBT states (full line) are represented.

ergies transitions from the VB to the D_B^+ states are involved (PB). Including these transitions between DB and band states, one obtains calculated spectra as represented by the full line in Fig. 3(a) and by the dashed line in Fig. 3(b). The ratios of the four coefficients in Eq. (5) are C_1:C_2:C_3:C_4 = 1.2:1.15:1.15:1.6. The high value of C_4 corresponds to the sharp decrease at the higher photon energies of the $-\Delta T/T$ spectra, ascribed to the $B_4^- \rightarrow$ CB transitions. In fact, also transitions from VBT states to the CB can contribute to this strong bleaching. Therefore, these transitions are possibly included in the term of $\Delta\alpha$ with coefficient C_4. Accounting for VBT states separately in the calculations, given by the extra terms in (10), results in the spectrum represented by the full line in Fig. 3(b). The bump appearing at lower photon energies may be due to the transitions between the VB and the VBT. Unfortunately, our experimental setup is not suited for measurements at these lower energies.

The calculated spectra which fit the low-temperature data of the sample with the lowest boron concentration are obtained with the Fermi level E_F positioned at 0.5 eV above the VB edge.[6,20] The quasi-Fermi level for trapped electrons E_{Fn} is shifted through the DB states to 1.5 eV and the quasi-Fermi level for trapped holes E_{Fp} is located at 0.15 eV. Because we assume as many B_4^- states are changed into B_4^0 states by trapping holes as D_B^+ states are transformed into D_B^0 states by trapping electrons, a level l=0.25 is used. As value for E_g, the Tauc gap increased by 0.15 eV has to be taken. Also in previous measurements on a-Si:H and a-Si:C:H alloys the effective gap for OMS was significantly larger than the Tauc gap, resulting in larger optical transition energies; this effect may be due to lattice relaxation. The B_4^- Gaussian distribution peaks at 0.25 eV, while the B_4^0 states are distributed around 0.45 eV. The standard deviation of both distributions is 0.04 eV; this order of magnitude is also adopted by others.[6,8] D_B^+ and D_B^0 states are located at 1.2 eV; the standard deviation of the Gaussians is given a value of 0.15 eV.[3,6,7] Where VBT states are involved in the calculations, a band-tail parameter E_0 = 0.05 eV is used.[7,8]

The room-temperature data of the same sample are shown in Fig. 4. A nice fit is obtained when shifting the quasi-Fermi level for trapped electrons towards E_F and by using a slightly smaller E_g value than the one at $T \simeq 20$ K. The parameters E_{Fp} and E_{Fn} are 0.15 eV and 1.2 eV, respectively. Compared to the positions of these levels at $T \simeq 20$ K, we can infer E_{Fp} is not shifted towards midgap while E_{Fn} is. This asymmetrical shift of the quasi-Fermi levels requires l=0.30. The E_{Fp} level is not moved because of the sharp distribution of the B_4 and VBT states. The E_g value at room temperature is the Tauc gap increased by 0.1 eV. No VBT states are involved in the fit represented by the dashed line. For this fit, the ratios of the four coefficients C_1:C_2:C_3:C_4 are 0.6:0.65:0.25:0.75. The largest change, compared to the values obtained at $T \simeq 20$ K, is observed in C_3, corresponding with the VB $\rightarrow$ D_B^+ transitions. This lower value indicates that these transitions are less probable at room temperature than at $T \simeq 20$ K. This effect is also clearly seen in Fig. 2. The energy positions of the dopant and the DB states as well as the widths of their Gaussian distributions are the same at high and low tem-

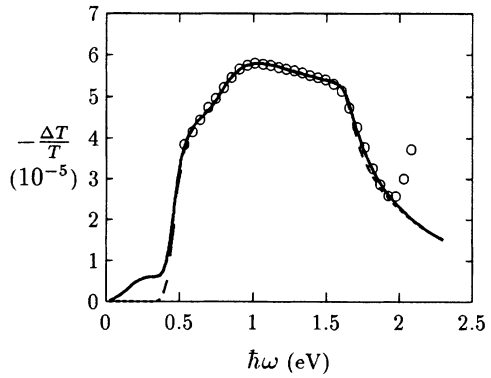

FIG. 4. Experimental (o) and calculated $-\Delta T/T$ spectra of the p-type a-Si:H sample with a (SiH_4:B_2H_6+H_2) ratio of (2:1) measured at room temperature. The curves are scaled so that the highest values coincide. Calculated spectra involving DB's and dopant states (dashed line) as well as the effect of the extra contribution of VBT states (full line) are represented.

peratures. Calculations involving VBT states result in the spectrum given by the full line. A similar bump as noticed at $T \simeq 20$ K, associated with VB $\rightarrow$ VBT transitions, is occurring at the lower photon energies. At the higher photon energies a better fit of the strong bleaching is obtained, indicating VBT $\rightarrow$ CB transitions are probable contributions.

One may wonder whether the values obtained for the fitting parameters are unique and whether it is possible to fit the data with other sets of parameter values. First of all, we will have a closer look at the energy positions of the band gap states. The experimental curves have some well-defined features, such as the onset of the bleaching contributions at about 1.2 eV, associated with the VB $\rightarrow D_B^+$ optical transition, and at about 1.6 eV, ascribed to the $B_4^- \rightarrow$ CB optical transition, as may be seen in Figs. 2 and 3. There is no way to obtain reasonable fits with energy parameters deviating more than $\pm$ 0.05 eV from the corresponding values of the transitions mentioned. The uncertainty on the energy position of the B_4^- states follows from the uncertainty on the gap energy E_g because we subtract the well-defined transition energy for the strong bleaching at 1.6 eV from E_g to obtain the energy position of B_4^- states with respect to the VB. As such, with an E_g value of about 1.85 eV, the B_4^- must be positioned at 0.25 eV above the VB. When keeping the D_B^0 and D_B^+ energy position at the same value, the gap energy parameter E_g is also fixed within $\pm$ 0.05 eV. Concerning the B_4^0 states, the determination of the energy position is less accurate because our experimental setup does not allow measurements below 0.5 eV. In spite of the larger uncertainty, it turns out that the PA transition energy involving B_4^0 states is always higher than 0.25 eV, corresponding to the energy position of the B_4^- with respect to the VB. Positioning the B_4^0 states at 0.45 eV gives reasonable fits with acceptable values for the C_i. Secondly, the standard deviations σ_i have been given values from literature; small variations do not greatly influence the above-mentioned parameters. Also the coefficients C_i are less unique: e.g., if we assign smaller values to the widths of the D_B^0 than to the D_B^+ distributions, reasonable fits can be obtained with adapted C_i. Because there is no immediate reason for this difference in distribution width we used the same σ_i values for all samples. Although the contributions of the valence band tail states and the boron states cannot precisely be separated, the above analysis shows that VBT states, with literature data for the parameters, slightly improve the fitting quality but they cannot replace the boron contributions totally. Concerning the room-temperature data, with smaller shifts of E_{Fp} compared to those at low temperature, comparable fits are obtained when involving dopant and DB states only; however, when adding VBT contributions, no reasonable fits of the strong bleaching at the higher photon energies could be achieved with these values of E_{Fp}. Therefore, we decide that the quasi-Fermi level for trapped holes is rather pinned.

TABLE I. Energy positions (with respect to the VB) of the dopant and dangling-bond states of the three B-doped a-Si:H samples. The values in parentheses represent the (SiH_4:B_2H_6+H_2) ratios.

Sample	$E(B_4^-)$ (eV)	$E(B_4^0)$ (eV)	$E(D_B^{+,0})$ (eV)
(2:1)	0.25	0.45	1.20
(1:1)	0.25	0.45	1.22
(1:2)	0.25	0.45	1.25

In order to obtain fits for the samples with higher boron concentration, E_g must be lowered corresponding to the decreasing optical gap with increasing doping (see Sec. III). Other parameters also have to be altered. The Fermi level E_F has not been changed because this parameter is only little dependent on boron doping in the investigated range.[20] Resulting energy positions are summarized in Table I. Calculations are made involving all gap states and with $\sigma(D_B^+) = \sigma(D_B^0)$. For the energy positions of the dangling-bond states a tendency to higher photon energies with increasing doping is observed. This observation is in agreement with results obtained by other groups using other experimental methods.[7,8] The B_4^- and B_4^0 states stay at the same energy level.

VI. CONCLUSIONS

A series of p-type a-Si:H samples have been studied by the OMS technique. Comparing the spectra with those of undoped a-Si:H, we notice that other states besides the Si dangling bonds play a role. Using the simplified model for the DOS distribution to obtain calculated spectra of the OMS data, it was found that also dopant states as well as VBT states contribute to the spectra. Furthermore, the energy positions of DB and dopant states are determined. The B_4^- states are located at 0.25 eV with respect to the VB, while the B_4^0 states are positioned at 0.45 eV. The dangling bonds have an energy position slightly shifting from 1.2 eV to 1.25 eV with increasing boron doping.

ACKNOWLEDGMENTS

The authors would like to thank Dr. W.G.J.H.M. van Sark and Dr. J. Bezemer of the University of Utrecht for providing them with the samples and Jan Jansen for helpful discussions about computer modeling. This research was supported by the Belgian Interuniversitair Instituut voor Kernwetenschappen (I.I.K.W.).

[1] W.E. Spear and P.G. LeComber, Solid State Commun. **17**, 1193 (1975).
[2] Z. Vardeny, T.X. Zhou, H.A. Stoddart, and J. Tauc, Solid State Commun. **65**, 1049 (1988).
[3] L. Chen, J. Tauc, J. Kočka, and J. Stuchlík, Phys. Rev. B **46**, 2050 (1992).
[4] J. Kočka, J. Stuchlík, M. Stutzmann, L. Chen, and J. Tauc, Phys. Rev. B **47**, 13 283 (1993).
[5] C.C. Tsai, Phys. Rev. B **19**, 2041 (1979).
[6] Jan Kočka, J. Non-Cryst. Solids **90**, 91 (1987); J. Kočka, M. Vaněček, and F. Schauer, *ibid.* **97&98**, 715 (1987).
[7] R. Kuntz and J. Dziesiaty, Phys. Status Solidi A **124**, K149 (1991); in this study tri-ethyl-bor (TEB) is used as doping gas but a comparison with B_2H_6-doped material is given.
[8] M.B. Schubert, G. Schumm, E. Lotter, K. Eberhardt, and G.H. Bauer, in *Amorphous Silicon Technology—1991*, edited by A. Madan, Y. Hamakawa, M. Thompson, P. C. Taylor, and P. G. LeComber, MRS Symposia Proceedings No. 219 (Materials Reserach Society, Pittsburgh, 1991), p. 551.
[9] P. O'Connor and J. Tauc, Phys Rev. B **25**, 2748 (1982).
[10] R. Ranganathan, M. Gal, and P.C. Taylor, Phys Rev. B **37**, 10 216 (1988).
[11] J. Tauc and Z. Vardeny, Philos. Mag. B **52**, 313 (1985).
[12] H.A. Stoddart, Z. Vardeny, and J. Tauc, Phys. Rev. B **38**, 1362 (1988).
[13] Z. Vardeny, T.X. Zhou, and J. Tauc, in *Amorphous Silicon and Related Materials*, edited by H. Fritzsche (World Scientific, Singapore, 1989), p. 513.
[14] W. Grevendonk, M. Verluyten, J. Dauwen, G.J. Adriaenssens, and J. Bezemer, Philos. Mag. B **61**, 393 (1990).
[15] R.A. Street, D.K. Biegelsen, and J.C. Knights, Phys. Rev. B **24**, 969 (1981).
[16] W.B. Jackson and N.M. Amer, Phys. Rev. B **25**, 5559 (1982).
[17] R.A. Street, Phys. Rev. Lett. **49**, 1187 (1982).
[18] G. Müller, H. Mannsperger, and S. Kalbitzer, Philos. Mag. B **53**, 257 (1986).
[19] R.A. Street, J. Kakalios, C.C. Tsai, and T.M. Hayes, Phys. Rev. B **35**, 1316 (1987).
[20] M. Stutzmann, D.K. Biegelsen, and R.A. Street, Phys. Rev. B **35**, 5666 (1987).
[21] K. Pierz, W. Fuhs, and H. Mell, Philos. Mag. B **63**, 123 (1991).
[22] P. O'Connor and J. Tauc, Solid State Commun. **36**, 947 (1980).